OXFORD
(GIGA)^n SCIENCE

GigaScience, 9, 2020, 1–13

doi: 10.1093/gigascience/giaa037
Data Note

DATA NOTE

The gene-rich genome of the scallop *Pecten maximus*

Nathan J. Kenny[1,2], Shane A. McCarthy[3], Olga Dudchenko[4,5], Katherine James[1,6], Emma Betteridge[7], Craig Corton[7], Jale Dolucan[7,8], Dan Mead[7], Karen Oliver[7], Arina D. Omer[4], Sarah Pelan[7], Yan Ryan[9,10], Ying Sims[7], Jason Skelton[7], Michelle Smith[7], James Torrance[7], David Weisz[4], Anil Wipat[9], Erez L Aiden[4,5,11,12], Kerstin Howe[7] and Suzanne T. Williams[1,*]

[1]Natural History Museum, Department of Life Sciences, Cromwell Road, London SW7 5BD, UK; [2]Present address: Oxford Brookes University, Headington Road, Oxford OX3 0BP, UK; [3]University of Cambridge, Department of Genetics, Cambridge CB2 3EH, UK; [4]The Center for Genome Architecture, Department of Molecular and Human Genetics, Baylor College of Medicine, Houston, TX 77030, USA; [5]The Center for Theoretical Biological Physics, Rice University, 6100 Main St, Houston, TX 77005-1827, USA; [6]Present address: Department of Applied Sciences, Faculty of Health and Life Sciences, Northumbria University, Newcastle upon Tyne NE1 8ST, UK; [7]Wellcome Sanger Institute, Cambridge CB10 1SA, UK; [8]Present address: Freeline Therapeutics Limited, Stevenage Bioscience Catalyst, Gunnels Wood Road, Stevenage, Hertfordshire, SG1 2FX, UK; [9]School of Computing, Newcastle University, Newcastle upon Tyne NE1 7RU, UK; [10]Institute of Infection and Global Health, Liverpool University, iC2, 146 Brownlow Hill, Liverpool L3 5RF, UK; [11]Shanghai Institute for Advanced Immunochemical Studies, Shanghai Tech University, Shanghai, China and [12]School of Agriculture and Environment, University of Western Australia, Perth, Australia.

[*]**Correspondence address**. Suzanne T. Williams, Department of Life Sciences, Natural History Museum, Cromwell Road, London SW7 5BD, UK. E-mail: s.williams@nhm.ac.uk http://orcid.org/0000-0003-2995-5823

Abstract

Background: The king scallop, *Pecten maximus*, is distributed in shallow waters along the Atlantic coast of Europe. It forms the basis of a valuable commercial fishery and plays a key role in coastal ecosystems and food webs. Like other filter feeding bivalves it can accumulate potent phytotoxins, to which it has evolved some immunity. The molecular origins of this immunity are of interest to evolutionary biologists, pharmaceutical companies, and fisheries management. **Findings:** Here we report the genome assembly of this species, conducted as part of the Wellcome Sanger 25 Genomes Project. This genome was assembled from PacBio reads and scaffolded with 10X Chromium and Hi-C data. Its 3,983 scaffolds have an N50 of 44.8 Mb (longest scaffold 60.1 Mb), with 92% of the assembly sequence contained in 19 scaffolds, corresponding to the 19 chromosomes found in this species. The total assembly spans 918.3 Mb and is the best-scaffolded marine bivalve genome published to date, exhibiting 95.5% recovery of the metazoan BUSCO set. Gene annotation resulted in 67,741 gene models. Analysis of gene content revealed large numbers of gene duplicates, as previously seen in bivalves, with little gene loss, in comparison with the sequenced genomes of other marine bivalve species. **Conclusions:** The genome assembly of *P. maximus* and its annotated gene set provide a high-quality platform for studies on such disparate topics as shell

Received: 18 January 2020; **Revised:** 26 February 2020; **Accepted:** 24 March 2020

biomineralization, pigmentation, vision, and resistance to algal toxins. As a result of our findings we highlight the sodium channel gene *Nav1*, known to confer resistance to saxitoxin and tetrodotoxin, as a candidate for further studies investigating immunity to domoic acid.

Keywords: scallop; bivalve; mollusc; genome; domoic; neurotoxin

Context

Scallops are bivalve molluscs (Pteriomorphia, Pectinida, Pectinoidea, Pectinidae; Fig. 1A and B), found globally in shallow marine waters, where their filter-feeding lifestyle helps perform a variety of ecological functions [1]. There are ∼400 living scallop species [2], and of these, *Pecten maximus* (Fig. 1A), also known as the king scallop, great scallop, and St James scallop, is perhaps the best-studied European species. *Pecten maximus* is found around the coast of western Europe from northern Norway to the Iberian Peninsula (Fig. 1C) where it is locally common in many areas, and it can occasionally be found more distantly in West Africa and on mid-North Atlantic islands [2]. It is commercially fished across its range, most heavily around France and the United Kingdom [3, 4], and is the most valuable single-species fishery in the English Channel with ∼35,000 tonnes of international landings reported in 2016 [4]. It has also been cultivated in aquaculture, particularly in the United Kingdom, Spain, Norway, and France, although with limited commercial production [5, 6]. It is an important part of the ecosystems within which it occurs, performing key roles in food webs, both as a prey species and more indirectly by cycling nutrients during filter feeding [1].

Previous studies in this species have aimed to elucidate its population dynamics, swimming behaviour, visual systems, and reproduction (e.g., [7–10]). Of particular interest to medicine, fisheries management, and molecular biology is the means by which this species is resistant to neurotoxins such as saxitoxin (STX) and domoic acid (DA). DA and STX are potent neurotoxins produced by certain species of phytoplankton, including dinoflagellates and diatoms, which may be present in large blooms [3]. Some shellfish (e.g., scallops, *P. maximus;* mussels, *Mytilus edulis*; cockles, *Cerastoderma edule*; razor clams, *Siliqua patula*), fish (e.g., anchovy, *Engraulis mordax*; European sardine, *Sardina pilchardus*; and Pacific halibut, *Hippoglossus stenolepis*), and crabs (e.g., *Cancer magister*) accumulate algal neurotoxins by filtration of phytoplankton or by ingestion of contaminated organisms, with species-specific accumulation rates [11–13]. In humans, ingestion of DA or STX has been associated with gastrointestinal and neurological symptoms [14, 15]. In severe cases, poisoning by DA may lead to death or permanent memory loss, a syndrome known as amnesic shellfish poisoning (ASP), and in the case of STX, paralysis (paralytic shellfish poisoning [PSP]) [16]. Curiously, however, shellfish and fish that routinely accumulate algal toxins are often able to do so without apparent effect on their health [17, 18]. The resistance of *P. maximus* in particular, and of bivalve molluscs more generally, to these potent toxins is of keen interest to fisheries groups, health care providers, and molecular biologists, yet the genetic mechanism behind this remains unknown. Detailed investigation into this phenomenon, along with many others, would be greatly aided by a genome resource.

At the time of writing, 9 bivalve genomes are available, with those of the Pacific oyster *Crassostrea gigas* [19] and the pearl oyster *Pinctada fucata* [20] in particular having been used for a variety of investigations into bivalve biology. Scallops have been the subject of genome sequencing projects in the past, with genomes published for 3 species, *Azumapecten farreri* (as *Chlamys*) [21] and *Mizuhopecten yessoensis* (as *Patinopecten*) [22] from the subfamily Pedinae, and *Argopecten purpuratus* from the subfamily Pectininae [23]. Other sequenced genomes for pteriomorph bivalves include those of the Sydney rock oyster *Saccostrea glomerata* [24], eastern oyster *Crassostrea virginica* (unpublished, but see [25]), and the mussels *Mytilus galloprovincialis* [26], *Limnoperna fortunei* [27], *Gigantidas platifrons* (as *Bathymodiolus*), and *Modiolus philippinarum* [28]. There are also extant resources for more distantly related bivalves including the razor clam *Sinonovacula constricta* [29], snout otter clam *Lutraria rhynchaena* [30], blood clam *Anadara broughtonii* (as *Scapharca*) [31], Manila clam *Ruditapes philippinarum* [32], and the freshwater mussels *Venustaconcha ellipsiformis* [33], *Dreissena rostriformis* [34], and *Dreissena polymorpha* (McCartney et al. [35]). Of these resources, only the assemblies for *S. constricta*, *C. virginica*, and *S. broughtonii* are of chromosomal quality, and the scaffold N50 of the other resources varies widely.

These studies demonstrate that bivalve genomes are often 1 Gb or more in size, and generally exhibit large amounts of heterozygosity, related to their tendency to be broadcast spawners with excellent dispersal capabilities, resulting in large degrees of panmixia. Gene expansion has been noted as a characteristic of the clade, with some species exhibiting tandem duplications and gene family expansions, particularly in genes associated with shell formation and physiology (e.g., HSP70 [36]).

Here we describe the genome of the king scallop, *P. maximus*, which has been assembled from Pacific Biosciences (PacBio), 10X Genomics, and Hi-C libraries. It is a well-assembled and complete resource and possesses a particularly large gene set, with duplicated genes making up a substantial part of this complement. This genome and gene set will be useful for a range of investigations in evolutionary genomics, aquaculture, population genetics, and the evolution of novelties such as eyes and colouration, for many years to come.

Methods

Sample information, DNA extraction, library construction, sequencing, and quality control

A single adult *Pecten maximus* (NCBI:txid6579; marinespecies.org:taxname:140712) was purchased commercially, marketed as having been collected in Scotland. The shell was preserved and is deposited in the Natural History Museum, London, with registration number NHMUK 20170376. The adductor muscle was used for high molecular weight DNA extraction using a modified agarose plug–based extraction protocol (Bionano Prep Animal Tissue DNA Isolation Soft Tissue Protocol, Bionano Genomics, San Diego, CA, USA). DNA was cleaned using a standard phenol/chloroform protocol (phenol: chloroform: isoamyl alcohol 25:24:1, followed by centrifugation and ethanol precipitation), concentration determined with a Qubit high sensitivity kit, and high molecular weight content confirmed by running on a Femto Pulse (Agilent, Santa Clara, CA, USA).

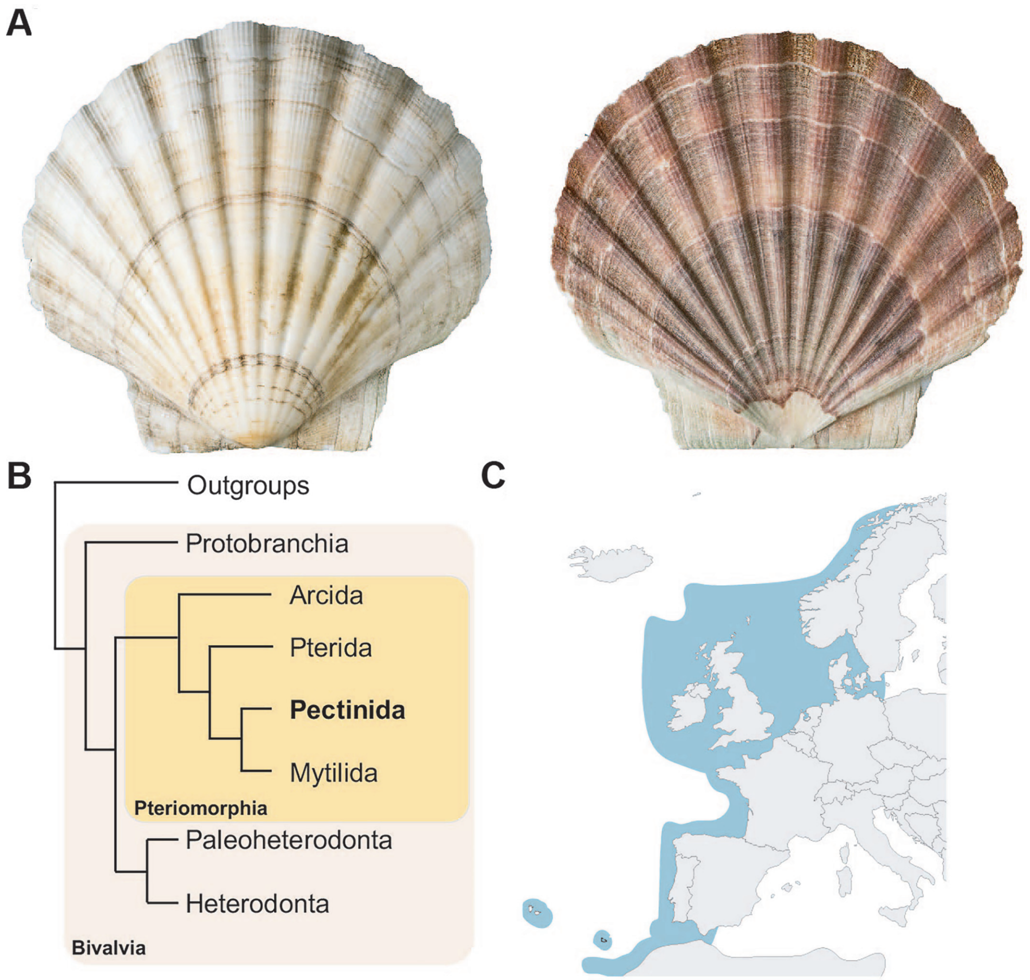

Figure 1: A, Photo of both valves of the shell of *Pecten maximus*, from the specimen sequenced in this work (NHMUK 20170376). B, Diagrammatic cladogram illustrating the phylogeny of the Bivalvia (after Gonzalez et al. [37]), showing the major sub-classes of Bivalvia and (boxed in yellow) the major divisions of the Pteriomorphia. *Pecten maximus* is a member of the superfamily Pectinoidea, which includes Pectinidae (scallops), Propeamussiidae (glass scallops), and Spondylidae (spiny oysters), and together with their close relatives (Anomioidea, jingle shells; Dimyoidea, dimyarian oysters; and Plicatuloidea, kittenpaw clams) these superfamilies form the order Pectinida. C, Distribution map of *P. maximus*, showing range (dark blue) of species across northern Europe and surroundings (map from simplemaps, distribution according to [2]).

PacBio and 10X Genomics linked-read libraries were made at the Wellcome Sanger Institute High-Throughput DNA Sequencing Centre by the Sanger Institute R&D and pipeline teams using established protocols. PacBio libraries were made using the SMRTbell Template Prep Kit 1.0 and 10X libraries using the Chromium Genome Reagent Kit (v2 Chemistry). These libraries were then sequenced on Sequel 1 and Illumina HiSeq X Ten platforms, respectively, at the Wellcome Sanger Institute High-Throughput DNA Sequencing Centre. The raw data are available from the European Nucleotide Archive, with accession number ERS3230380. Hi-C reads were created by the DNA Zoo Consortium (www.dnazoo.org) and submitted to NCBI with accession number SRX6848914. Read quality, adapter trimming, and read length were assayed using NanoPlot and NanoComp (PacBio reads) [38] and FastQC (10X reads, FastQC, RRID:SCR_014583) [39] (Supplementary File 1 [40, 41]). PacBio libraries provided ~65.9× coverage of this genome; 10X reads and Hi-C provided a further 113.7× and 63.4× estimated coverage, respectively, assuming a genome size of 1.15 Gb as estimated from our reads (see Fig. 2). A summary of statistics relating to these reads can be found in Table 1.

Genome assembly

PacBio reads were first assembled with wtdbg2 v2.2 using the ”-xsq” preset option for PacBio Sequel data [42]. The PacBio reads were then used to polish the contigs using Arrow (genomic-consensus package, PacBio tools). This was followed by a round of Illumina polishing using the 10X data, which consisted of aligning the 10X data to the contigs with longranger align, calling variants with freebayes (freebayes, RRID:SCR_010761) 1.3.1 [43] and applying homozygous non-reference edits to the assembly using bcftools-consensus [44]. Medium-range scaffolding was performed using Scaff10X v.4.2 [45]. Longer-range Hi-C–based scaffolding was then performed on the 10X assembly by the DNA Zoo Consortium using 3D-DNA [46], followed by manual curation of difficult regions by means of Juicebox Assembly Tools [47]. A further round of polishing with Arrow was performed on the resulting scaffolds, with reads spanning gaps contributing to filling in assembly gaps. This was followed by a further 2 rounds of freebayes (freebayes, RRID:SCR_010761) Illumina polishing. Finally, the assembly was analysed and manually curated by inspection using the gEVAL browser [48].

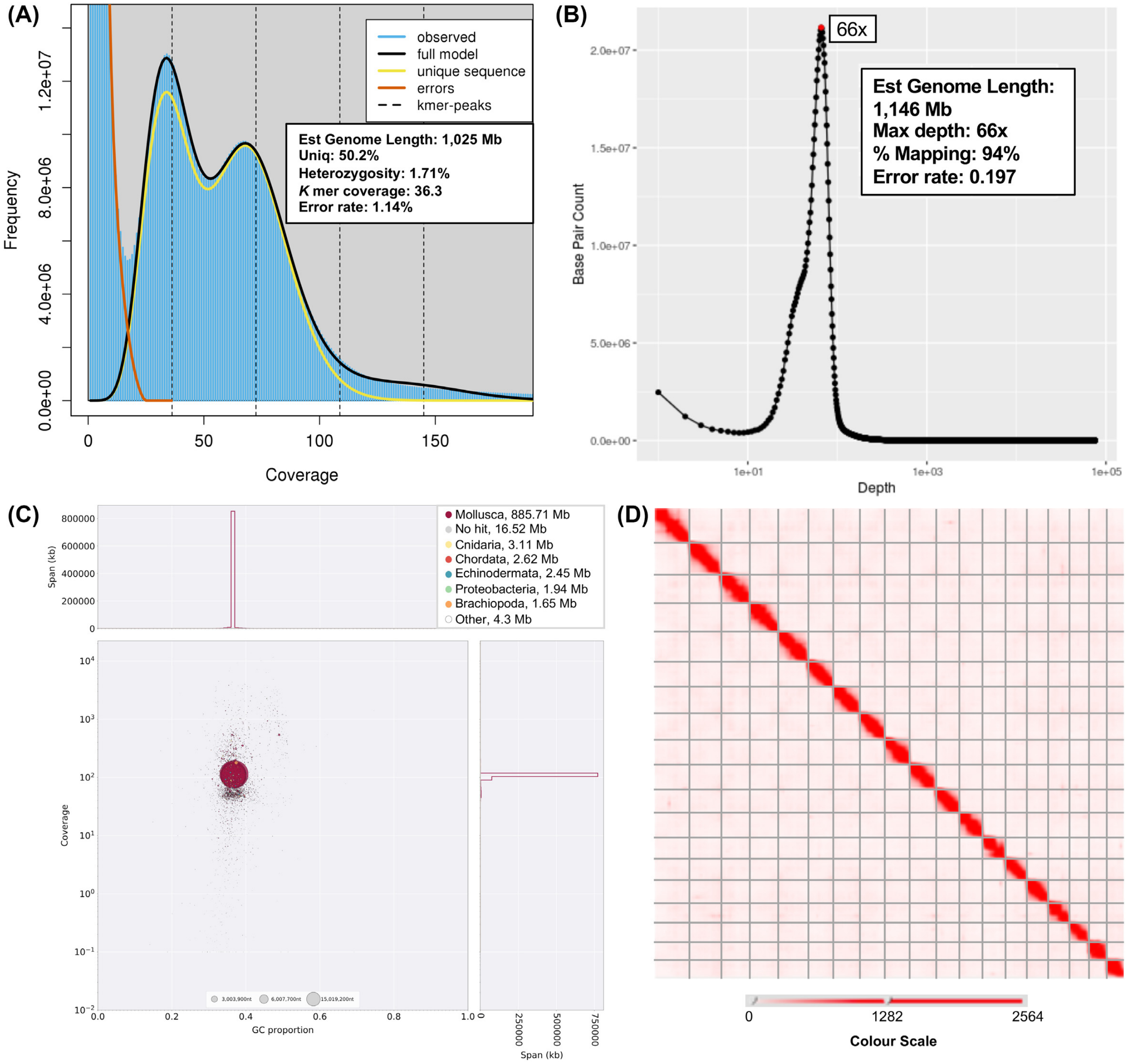

Figure 2: A, Genomescope2 [49] plot of the 21-mer *k*-mer content within the *Pecten maximus* genome. Models fitted and resulting estimates of genome size and read data as shown on figure. B, Base pair count by depth in PacBio data, determined using PBreads/Minimap2. C, Blobplot [50] of content of the *P. maximus* genome. Note that little-to-no contamination of the assembly can be observed, with the small amount of sequence annotated as non-metazoan mirroring the metazoan content in GC content and average coverage. Additional Blobplot plots and data, including those separated by phylum/superkingdom, can be found in Supplementary File 2. D, Hi-C contact map based on assembly created using 3D-DNA and Juicebox Assembly Tools (see [51] for an interactive version of this panel).

Table 1: Libraries sequenced and used in assembly, with accession numbers

Library type	No. of sequencing runs	No. of reads	No. of bases (Gb)	GC %	Nominal coverage (1.15 Gb genome)	Accessions
10X	4	433,117,392	130.8	39.5	113.7×	ERR3316025–ERR3316028
PacBio	13	7,246,290	75.8	39.0	65.9×	ERR3130278–ERR3130281, ERR3130284–ERR3130292
Hi-C	1	241,297,364	72.9	38.7	63.4×	SRX6848914

Full statistics regarding our assembly can be seen in Table 2. The assembly contains a total of 918,306,378 bp, across 3,983 scaffolds. The N50 is 44,824,366 bp, with 50% of the genome found in 10 scaffolds. The Hi-C analysis identified that P . *maximus* possesses 19 pairs of chromosomes, in agreement with a prior study [52], and these are well recovered in our assembly, with 844,299,368 bp (92%) of our assembly in the 19 biggest scaffolds, the smallest of which is 32,483,354 bp, and

Table 2: Basic metrics relating to assembled genome

Total assembly length (bp)	918,306,378
GC content of scaffolds	36.62%
Maximum scaffold length (bp)	60,076,705
N50 scaffold length (bp)	44,824,366
N90 scaffold length (bp)	32,483,354
No. of scaffolds	3,983
No. of scaffolds in N50	10
No. of chromosomes	19
% genome, chromosome-length scaffolds	92%
N content, total (bp)	691,874

the largest 60,076,705 bp in length; only 0.08% of the assembly is represented as Ns (691,874 bp). The assembly was screened for trailing Ns, and for contamination against databases of common contamination sources, adapter sequences, and organelle genomes derived from NCBI (using megaBLAST algorithm, requiring *e*-value ≤1e−4, sequence identity ≥90%, and for organelle genome comparisons, match length ≥500 [53]). This process identified no contamination. The Hi-C contact map for the final assembly (Fig. 2D) demonstrates the integrity of the chromosomal units. The interactive version of the contact map is available at [51] (powered by Juicebox.js [54]) and on the DNAzoo website [55]. Our assembly is the most contiguous of all published bivalve genome assemblies to date (Table 3).

Assembly assessment

The total size of our assembly, 918 Mb, falls short of previous estimates of the genome size of *P. maximus,* with flow cytometry estimating a genomic C-value of 1.42 [56]. Assessments of genome size based on *k*-mer counting using Genomescope (10,000 cov cut-off) [57] suggest that the complete genome size is ~1.025 Gb (Fig. 2A). Estimates using PacBio reads and Minimap2 [58], showing base pair count at each depth, put the genome size at 1,146 Mb, which is more in line with flow cytometry results. This discrepancy is likely to be caused by heterochromatic regions inaccessible to current sequencing technologies.

The expected genome size of *P. maximus* is slightly larger than many other sequenced bivalve species, and our assembly size (in base pairs) is in line with that of other sequenced scallop species (Table 3). It is, however, half the size of the genomes of the sequenced mussels *G. platifrons* and *M. philippinarum*. Scallops therefore have intermediate genome sizes on average when compared to other molluscs - larger than oysters such as *C. gigas* and gastropods such as *Lottia gigantea,* but smaller than mussels and cephalopods. The reasons for these differences in genome size are at present unclear but may include gene duplications, repetitive element expansions, and, in some cases, whole-genome duplications (WGDs) [59].

To confirm the efficacy of the contamination screen performed during the assembly process, we verified the absence of parasitic or pathogenic sources by creating a Blobplot (Fig. 2C) using Blobtools (Blobtools, RRID:SCR_017618) [50]. We observed very few scaffolds (1.94 Mb, or ~0.21% of our assembly) with blast similarity to Proteobacteria, but with coverage values and GC content exactly mirroring the rest of the assembly. In the majority of these cases, the assignment to Proteobacteria will be due to a chance blast match with high similarity over a small region of the contig length, rather than actual bacterial origin (Supplementary File 2 [40, 41]). The vast majority of the assembly (885.71 Mb) was assigned to the clade Mollusca, as expected (Fig. 2C).

To assay assembly quality and completeness, we mapped our raw reads to the genome. Of the 10X Genomics paired-end reads, 94% (8.14×10^8 of 8.66×10^8 reads) mapped concordantly. Of our PacBio reads, 94% (71.13×10^9 of 75.7×10^9 bases) also mapped (Fig. 2B), indicating a well-assembled dataset, and one with little missing data.

The reasonably high level of observed heterozygosity calculated by GenomeScope (GenomeScope, RRID:SCR_017014) [57] from raw reads (1.71%, Fig. 2A) in the *P. maximus* assembly is a common phenomenon in broadcast-spawning marine invertebrates [60]. It should be noted that we used freebayes-polish on our final assembly when using this resource for studies focusing on genetic diversity, and no detectable heterozygosity will remain. In our raw reads, levels of heterozygosity in *P. maximus* were higher than those found in the Sydney rock oyster *Saccostrea* (0.51%), or the Pacific oyster *C. gigas* (0.73%). Both of these oyster samples were derived from selective breeding programmes, which would reduce heterozygosity compared to wild populations [24].

Repetitive elements have been noted as playing an important role in genome evolution in molluscs, and in bivalves in particular (e.g., [61]). We used RepeatModeler (RepeatModeler, RRID:SCR_015027) and RepeatMasker (RepeatMasker, RRID:SCR_012954) [62] to identify and mask regions of the genome containing previously identified or novel repetitive sequences (Table 4). With the caveat that not all repetitive elements have been classified, it seems that long terminal repeats (LTRs) are less common in *P. maximus* compared to other species (0.52%, cf. 1.35% in *S. glomerata* and 2.5% in *C. gigas*) but that short interspersed nuclear elements (SINEs) are more common (2.19%, cf. 0.09% in *S. glomerata* and 0.6% in *C. gigas*). A total of 27.0% of the genome was classified as repetitive elements, with 16.7% of the genome made up of elements not present in preconfigured RepeatMasker libraries (but likely shared with other bivalve species). While the genome of *P. maximus* is large by scallop standards, its size is not due to large amounts of repetitive elements because 27.0% is low compared to many other genome resources. For example, *C. gigas* has a repeat content of 36% [19], and *S. glomerata*, 45.0% [24].

Gene prediction and annotation

Gene sequences were predicted using Augustus (Augustus: Gene Prediction, RRID:SCR_008417) annotation software [63], with 1 novel [40, 41] and several previously published *P. maximus* RNA sequencing (RNAseq) datasets [64, 65] used for training. The novel dataset was derived from 2 samples of *P. maximus* mantle tissue from the same specimen used for genomic DNA extraction. These were sequenced on an Illumina HiSeq to a depth of 338,910,597 reads. After initial trimming of poor-quality sequence and residual adapters with TrimGalore v0.6 [66], this library was assembled using Trinity (Trinity, RRID:SCR_013048) v2.8.4 [67] with all default settings. Following assembly, chimeric, fragmented, or locally misassembled transcripts were filtered using Transrate v1.0.3 [68], where ”good” transcripts were retained, followed by DETONATE (DETONATE, RRID:SCR_017035) v1.11 with the bowtie2 option [69], where transcripts scoring <0 were discarded. Transcripts were then clustered using cd-hit-est v4.8.1 [70] at an identity threshold of 95% (-c 0.95 -n 8 -g 1), and the representative sequence of each cluster was retained. The non-masked genome was used as the basis for gene prediction, to avoid artefacts, missed exons, or missing gene portions caused by gene overlap with masked areas of the genome. Training was first performed using the aforementioned RNAseq datasets, as part of the AUGUSTUS pipeline (which incorporates BLAT alignment [71]). After training, the re-

Table 3: Genomic assemblies of a number of marine bivalves, and summary statistics relating to these assemblies

Family	Species	GC content (%)	Assembled length (Mb)	No. of scaffolds	Longest scaffold (Mb)	Scaffold N50 (Mb)	No. of missing BUSCOs (%)	Source
Pectinidae	*Pecten maximus*	37	918.3	3,983	60.1	44.8	44 (4.5)	This work
Pectinidae	*Azumapecten farreri*	35	779.9	96,024	6.5	0.6	53 (5.5)	[21]
Pectinidae	*Argopecten purpuratus*	35	724.8	89,727	11.1	1.0	36 (4.2)	[23]
Pectinidae	*Mizuhopecten yessoensis*	34	987.6	82,659	7.5	0.8	53 (5.5)	[22]
Mytilidae	*Gigantidas platifrons*	30	1,658.2	65,662	2.8	0.3	38 (3.9)	[28]
Mytilidae	*Modiolus philippinarum*	32	2,629.6	74,573	0.7	0.1	55 (5.6)	[28]
Pteriidae	*Pinctada fucata*	33	815.3	29,306	1.3	0.2	45 (4.6)	[20, 36]
Ostreidae	*Crassostrea gigas*	30	557.7	7,659	2.0	0.4	38 (3.9)	[19]
Ostreidae	*Saccostrea glomerata*	33	788.1	10,107	7.1	0.8	56 (6.7)	[24]

These data, with comparison to Gastropoda, can be seen in Table 1 of Sun et al. [72].

Table 4: Repeat content of the *P. maximus* genome based on RepeatModeler and RepeatMasker analysis

Element	Count	Length occupied (bp)	% of genome
SINEs	125,121	20,067,275	2.19
MIRs	21,406	3,059,644	0.33
LINEs	86,373	26,983,591	2.94
LINE1	803	463,519	0.05
LINE2	4,883	2,601,659	0.28
L3/CR1	4,374	1,588,697	0.17
LTR elements	9,334	4,731,793	0.52
DNA elements	121,409	31,845,557	3.47
hAT-Charlie	1,312	394,533	0.04
TcMar-Tigger	4,548	1,478,364	0.16
Unclassified	612,341	153,700,734	16.74
Total interspersed repeats		237,328,950	25.84
Small RNA	4,096	563,615	0.06
Simple repeats	174,931	9,099,659	0.99
Low complexity	25,658	1,411,700	0.15
Total length (of 918.3 Mb):		247,513,725	26.95

sulting hints file was submitted once more to Augustus for prediction, with options regarding untranslated regions (UTRs) and gene prediction on both strands set to "true." The same messenger RNA files used for initial training were also provided to AUGUSTUS for this prediction step. Note that UTR prediction with AUGUSTUS is imperfect in non-model organisms, and UTR regions provided here are current best estimates and would benefit from full-length RNA sequencing (e.g., Isoseq, on the PacBio platform).

This annotation resulted in an initial set of 215,598 putative genes (with 32,824 genes having ≥2 alternative isoforms), resulting in 249,081 discrete transcript models. We filtered the initial gene set by comparing our gene models to 7 previously published bivalve resources (*A. purpuratus, A. farreri, M. yessoensis, C. gigas, P. fucata, G. platifrons*, and *M. philippinarum*) using Orthofinder2 (OrthoFinder, RRID:SCR_017118), and retained genes with orthologues shared with other species (57,574 genes, further details below). To ensure that we did not discard transcribed genes absent from other bivalves but present in our resource, we also retained those genes with an empirically determined "good" hit in the *nr* database, lenient enough to recover genes from more distantly related species but stringent enough to avoid chance similarity (23,541 genes, diamond blastp, –more-sensitive –max-target-seqs 1 –outfmt 6 qseqid sallseqid stitle pident evalue –evalue 1e-9 [73]), a total of 81,115 genes. However, we then removed from this combined total any genes that had a match within our identified repetitive elements (13,374 genes, tblastn, -evalue 1e-29 -max_target_seqs 1 -outfmt '6 qseqid staxids evalue' [53]). This evalue cutoff was chosen after initial trials to include genes that mapped to *pol, env, tc3 transposase, Gag-Pol*, and *reverse transcriptase* genes in automated blast. This resulted in a final, 67,741-gene, curated set, of which 16,693 genes possess ≥1 alternative transcript. Full, curated and annotated gene sets in a variety of formats can be found in online repositories [40, 41].

This number, while still high in comparison to the number of genes found in many metazoan species, is comparable to the number of unigenes (72,187) in the *Argopecten irradians* resource [74]. To confirm the veracity of these gene models as transcribed genes, we mapped samples from a number of previously sequenced, independent RNAseq experiments to our gene models using STAR 2.7 [75] and the –quantMode GeneCounts option. This records only the reads corresponding to 1 gene, with no multimappers recorded, and is thus a highly stringent test of transcription. Of our 67,741 curated "high-confidence" gene models, 47,159 (69.6%) were transcribed in the novel mantle-specific RNA dataset presented in this article. From independent samples, 33,553 genes were transcribed in the mantle of the sole control sample from a previous heat stress experiment [64]. A total of 48,882 genes were expressed in 2 replicate late veliger controls from an experiment where embryos were exposed to a range of water conditions (varying pH, PRJNA298284) and 39,640 were expressed in MiSeq reads sampled from mixed adductor muscle, hepatopancreas, and male and female gonad tissue (PRJEB17629). In total, 57,368 of our 67,741 curated high-confidence gene models (84.7%) are supported by these independent RNAseq experiments, 54,153 (79.9%) of which were found in samples other than our novel transcriptome. These mapping results have been made available for download as Supplementary File 3 (40, 41. It should be noted that this is likely an underestimate of transcription, given that multi-mapping reads were discounted from consideration. If additional tissues and life stages were targeted, given the fact that these genes have known orthologues in closely related species (see Orthofinder2 results above), it is likely that almost all of our gene models would be found to be expressed.

The 84,866 transcripts in our high-confidence gene set (some genes possess >1 transcript) have a mean of 5 exons. This is fewer than that seen in *M. yessoensis* (7 exons on average) or *P. fucata* (6 on average) (Table S8, [22]). This may indicate a degree of fragmentation in our gene models (although that is not observed empirically), or alternatively, that some of the genes in our gene models have been copied via retrotransposition and lack introns, which would lower the average exon number and contribute to the high number of genes seen in this species.

We assayed the completeness of our gene set using BUSCO v2 (BUSCO, RRID:SCR_015008) [76], using metazoan gene sets. Of the 978-gene Metazoa dataset, 924 (94.5%) complete BUSCOs (of which 32 [3.3%] were duplicated), 10 incomplete (1.0%) BUSCOs, and 44 (4.5%) missing BUSCOs were recorded in genome mode, equating to a recovery of 95.5% of the entire BUSCO set. This is comparable to previously published bivalve resources (Table 3).

We have performed annotation of gene complements using 2 automated methods. BLAST annotation was performed with peptide sequences using DIAMOND against the *nr* database (locally updated 11 November 2019) with more lenient settings than used for curation of our gene models (tblastn, –more-sensitive –max-target-seqs 1 –outfmt 6 qseqid sallseqid stitle pident evalue –evalue 1e-3 –threads 4 [73]), with 88,824 of our unfiltered gene models recovering a hit, although this figure includes hits to repetitive elements removed in our curated dataset (Supplementary File 4, 40, 41). Of the 67,741 high-confidence genes, 59,772 possess a hit in the nr database (88.2%), indicating a highly annotatable dataset. We also used the KEGG-KAAS automatic annotation server, using peptide sequence and the Bidirectional Best Hit (BBH) method. The standard eukaryotic species set, complemented with *L. gigantea*, *Pomacea canaliculata*, *C. gigas, M. yessoensis*, and *Octopus bimaculoides* was used for annotation, with 14,495 of our gene models mapping to KEGG pathways (Supplementary File 5, 40, 41).

Gene complement and expansion

We investigated the gene complement of *P. maximus* to understand the nature of the events that resulted in it and other scallops possessing a large number of annotated genes compared with related mollusc species. This analysis was performed predominantly using Orthofinder2 (-t 8 -a 8 -M msa -T fasttree settings and using only the longest transcript per gene for *P. maximus,* Fig. 3A). These statistics reveal that *P. maximus* exhibits little gene loss compared with other related species. The percentage of orthogroups containing *P. maximus* genes is very high (83.4%) compared to every other species examined. *Pecten maximus* has therefore lost fewer genes from the ancestrally shared cassette than any of the other species listed. *Pecten maximus* also possesses 518 species-specific orthogroups—comparatively more than any other species listed. These genes could be true novelties because they are not found in any of the 8 other species of bivalve examined here, but they may be derived from repetitive content, as the unfiltered *P. maximus* gene set was used as the basis of this comparison.

Using these results, we are also able to understand the prevalence of gene duplication across the phylogeny of bivalves. Gene duplication events were inferred from the orthogroup analysis and mapped onto the phylogeny of the 8 bivalve species examined here (Fig. 3B). We conclude that gene duplication events are common in extant species of bivalve, and some gene duplicates are shared by leaf nodes as a result of events in the stem lineage. However, duplications in *P. maximus* are particularly prevalent. With 28,880 unique duplications, *P. maximus* has more than double the number of duplicates of any other species, with *M. yessoensis* the next closest example. However, it should be noted that not all gene annotations were performed in an identical fashion, and particularly if genes have been missed in other species, e.g., through sparse RNAseq for gene prediction, this will negatively influence their counts in these results.

Of the genes that are shared with other lineages, *P. maximus* has a highly complete complement (Fig. 3C). No other species examined here possesses as many shared orthogroups in total or shares as many with other species. In pairwise comparisons, only the mussels *M. philippinarum* and *G. platifrons* show similar numbers of shared orthogroups with each other, but not with other species. This is consistent with the previous finding that the scallop *M. yessoensis* is closer in gene complement to the oysters *C. gigas* and *P. fucata* than the oysters are to one another [22], a fact reflected in early divergence of these 2 distantly related oyster species [77]. Scallops in general therefore have a better-conserved gene cassette compared to the ancestral genotype than exhibited in oysters.

We conclude that *P. maximus* has a well-conserved gene set, which has been added to substantially by gene duplication. Its large gene complement is therefore explained by a strong pattern of gene gain, coupled to very little gene loss.

Hox genes

The prevalence of gene duplication within *P. maximus* led us to consider whether a WGD event had occurred in this lineage. As a test for this, we used the well-conserved Hox and Parahox gene clusters, which are normally preserved as intact complexes and duplicated in the presence of additional WGD events (e.g., [78, 79]).

P. maximus possesses a single Hox cluster spanning nearly 1.73 Mb (from 28,829,013 to 30,558,725 bp) on scaffold HiC_scaffold_2_arrow_ctg1 (Fig. 4A). It also features a single Parahox cluster on scaffold HiC_scaffold_5_arrow_ctg1. The complex, like that of *M. yessoensis* [22], is stereotypical. This evidence, along with a lack of any obvious signal in our *k*-mer plots (Fig. 2) or previous karyotypic work [52], suggests that no WGD has taken place, although this possibility cannot be completely excluded.

Immunity to neurotoxins

Bivalves are known to accumulate a number of toxins derived from phytoplankton, and human ingestion of contaminated bivalves can result in 5 known syndromes: ASP caused by DA, PSP from STX, diarrhetic shellfish poisoning from okadaic acid and analogues, neurotoxic shellfish poisoning caused by brevetoxin and analogues, and azaspiracid shellfish poisoning from azaspiracid [16]. Adult *P. maximus* are relatively immune to STX and DA and, as such, may be vectors for the syndromes PSP and ASP, which are of the greatest concern to human health [80, 81].

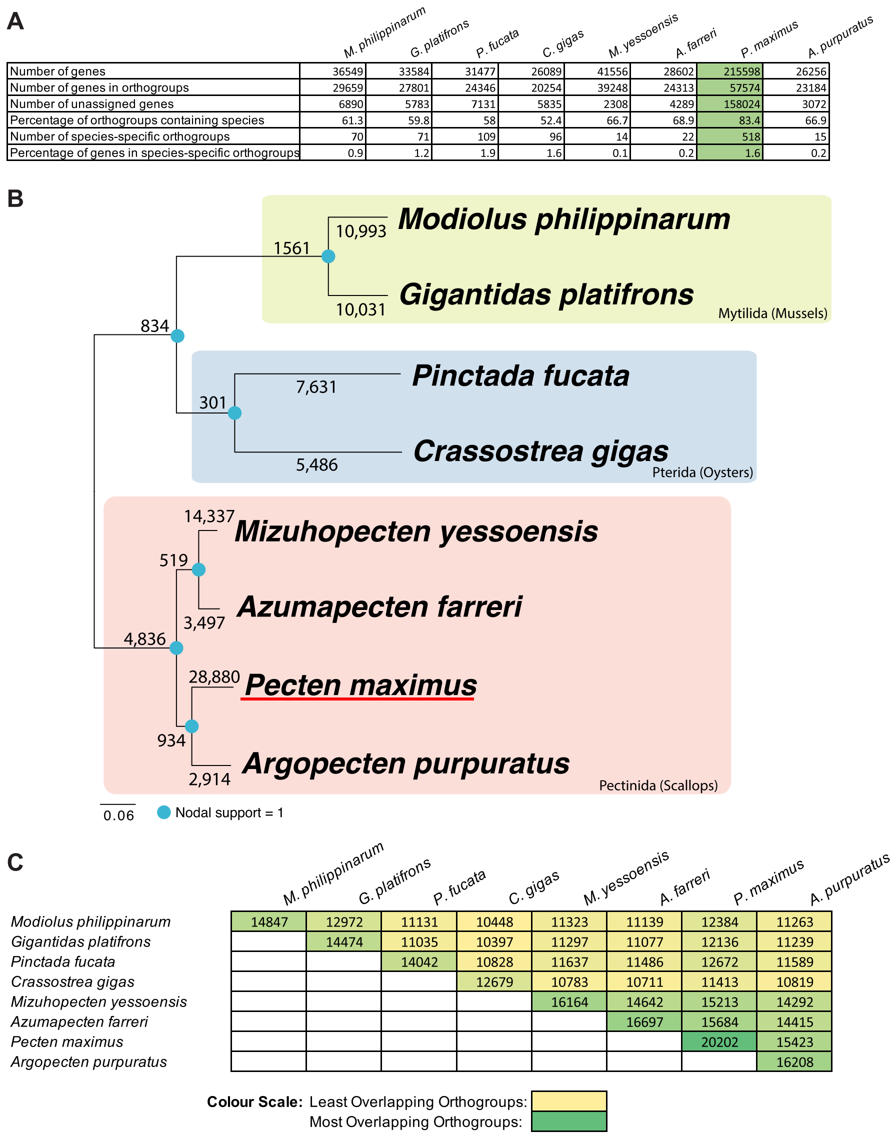

A

	M. philippinarum	*G. platifrons*	*P. fucata*	*C. gigas*	*M. yessoensis*	*A. farreri*	*P. maximus*	*A. purpuratus*
Number of genes	36549	33584	31477	26089	41556	28602	215598	26256
Number of genes in orthogroups	29659	27801	24346	20254	39248	24313	57574	23184
Number of unassigned genes	6890	5783	7131	5835	2308	4289	158024	3072
Percentage of orthogroups containing species	61.3	59.8	58	52.4	66.7	68.9	83.4	66.9
Number of species-specific orthogroups	70	71	109	96	14	22	518	15
Percentage of genes in species-specific orthogroups	0.9	1.2	1.9	1.6	0.1	0.2	1.6	0.2

B

C

	M. philippinarum	*G. platifrons*	*P. fucata*	*C. gigas*	*M. yessoensis*	*A. farreri*	*P. maximus*	*A. purpuratus*
Modiolus philippinarum	14847	12972	11131	10448	11323	11139	12384	11263
Gigantidas platifrons		14474	11035	10397	11297	11077	12136	11239
Pinctada fucata			14042	10828	11637	11486	12672	11589
Crassostrea gigas				12679	10783	10711	11413	10819
Mizuhopecten yessoensis					16164	14642	15213	14292
Azumapecten farreri						16697	15684	14415
Pecten maximus							20202	15423
Argopecten purpuratus								16208

Colour Scale: Least Overlapping Orthogroups: 🟨
Most Overlapping Orthogroups: 🟩

Figure 3: A, Orthofinder 2 [82] ortholog analysis of 8 sequenced marine bivalve species. *Pecten maximus* results shown in green. B, Phylogeny of bivalves using available marine bivalve genomes (generated from ortholog groups by STAG and displayed in Figtree), with root placed at midpoint. Blue dots indicate nodal support (=1 at every node). Numbers on internal nodes represent ancestrally shared duplications at the point of diversification. Numbers on leaf nodes indicate duplication events occurring solely in that taxon. C, Matrix showing numbers of overlapping orthogroups shared by the species examined. A colour scale has been applied to aid in identifying the most- and least-overlapping data sources.

STX and brevetoxin are neurotoxins that bind to the voltage-gated sodium channel, blocking the passage of nerve impulses [83]. Previous studies have shown that genetic mutations within the sodium channel gene, *Neuron Navigator 1* (*Nav1*), confer immunity in taxa that accumulate STX (e.g., the soft-shell clam *Mya arenaria* [84], scallop *Azumapecten farreri* [21], and copepods *Calanus finmarchicus* and *Acartia hudsonica* [85]) or other similar-acting neurotoxins such as tetrodotoxin (TTX) (e.g., pufferfish, *Tetraodon nigroviridis* and *Takifugu rubripes*; salamanders [86–89]; and the venomous blue-ringed octopus [90]).

The *P. maximus Nav1* gene possesses the expected canonical domain structure observed in other taxa. Furthermore, it possesses the characteristic thymine residue in Domain 3 (Fig. 5, position 1,425 in reference to rat sodium channel IIA), also described in the other 2 scallop species sequenced so far, which has been shown to confer resistance to these toxins in pufferfish, copepods, and the venomous blue-ringed octopus [85–87]. It does not, however, have the E945D mutation seen in the soft-shell clam *M. arenaria* and some pufferfish, which experimental evidence suggests also confers resistance [84], nor the D1663H or G1664S mutations in the blue-ringed octopus [90]. Instead, it has 1 novel and 2 ancestrally shared changes (shared with scallops and other bivalves) that may be of interest in studying alternative means of resistance in this molecule.

Unlike STX and TTX, DA does not directly target sodium channels; instead it mimics glutamate and binds preferentially to glutamate receptors including N-methyl-D-aspartate (NDMA), kainate, and α-amino-3-hydroxy-5-methyl-4-isoxazolepropionic acid (AMPA) receptors, leading to elevated levels of intracellular calcium and potentially, calcium toxicity

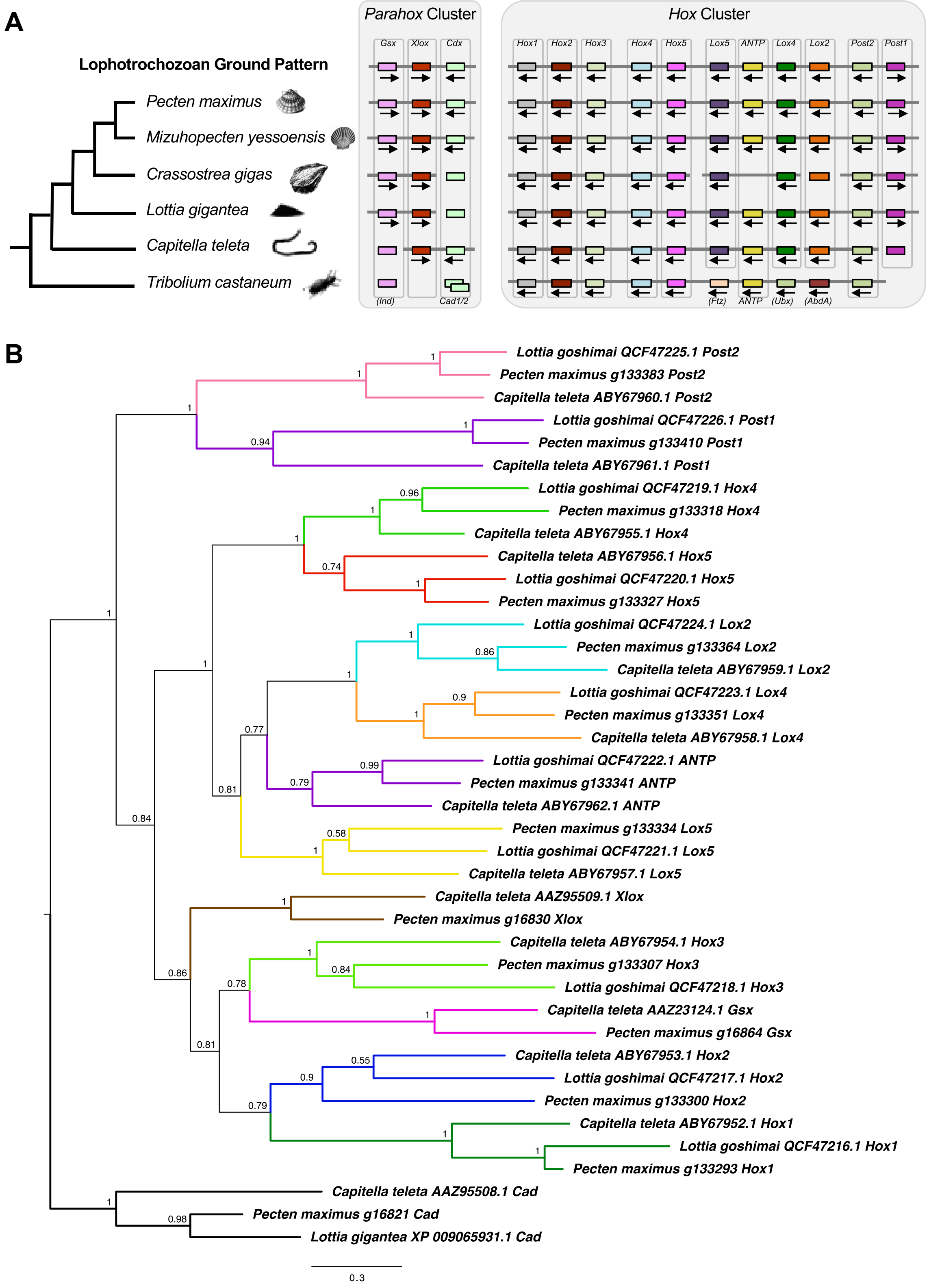
A
Lophotrochozoan Ground Pattern
Pecten maximus
Mizuhopecten yessoensis
Crassostrea gigas
Lottia gigantea
Capitella teleta
Tribolium castaneum
Parahox Cluster
Gsx
Xlox
Cdx
(Ind)
Cad1/2
Hox Cluster
Hox1
Hox2
Hox3
Hox4
Hox5
Lox5
ANTP
Lox4
Lox2
Post2
Post1
(Ftz)
ANTP
(Ubx)
(AbdA)
B
Lottia goshimai QCF47225.1 Post2
Pecten maximus g133383 Post2
Capitella teleta ABY67960.1 Post2
Lottia goshimai QCF47226.1 Post1
Pecten maximus g133410 Post1
Capitella teleta ABY67961.1 Post1
Lottia goshimai QCF47219.1 Hox4
Pecten maximus g133318 Hox4
Capitella teleta ABY67955.1 Hox4
Capitella teleta ABY67956.1 Hox5
Lottia goshimai QCF47220.1 Hox5
Pecten maximus g133327 Hox5
Lottia goshimai QCF47224.1 Lox2
Pecten maximus g133364 Lox2
Capitella teleta ABY67959.1 Lox2
Lottia goshimai QCF47223.1 Lox4
Pecten maximus g133351 Lox4
Capitella teleta ABY67958.1 Lox4
Lottia goshimai QCF47222.1 ANTP
Pecten maximus g133341 ANTP
Capitella teleta ABY67962.1 ANTP
Pecten maximus g133334 Lox5
Lottia goshimai QCF47221.1 Lox5
Capitella teleta ABY67957.1 Lox5
Capitella teleta AAZ95509.1 Xlox
Pecten maximus g16830 Xlox
Capitella teleta ABY67954.1 Hox3
Pecten maximus g133307 Hox3
Lottia goshimai QCF47218.1 Hox3
Capitella teleta AAZ23124.1 Gsx
Pecten maximus g16864 Gsx
Capitella teleta ABY67953.1 Hox2
Lottia goshimai QCF47217.1 Hox2
Pecten maximus g133300 Hox2
Capitella teleta ABY67952.1 Hox1
Lottia goshimai QCF47216.1 Hox1
Pecten maximus g133293 Hox1
Capitella teleta AAZ95508.1 Cad
Pecten maximus g16821 Cad
Lottia gigantea XP 009065931.1 Cad
1
1
1
0.94
1
0.96
1
1
0.74
1
1
1
0.86
1
0.9
1
0.77
0.99
0.79
0.81
0.84
0.58
1
1
0.86
1
0.84
0.78
1
0.81
0.55
0.9
0.79
1
1
1
0.98
0.3

Figure 4: A, Diagrammatic representation of Hox and Parahox cluster chromosomal organization showing a shared pattern among selected Lophotrochozoan taxa (scallops *Pecten maximus* and *Mizuhopecten yessoensis*, Pacific oyster *Crassostrea gigas*, owl limpet *Lottia gigantea*, and annelid *Capitella teleta*) along with an outgroup (red flour beetle [*Tribolium castaneum*]). Grey bar linking genes represents regions of synteny. Silhouette sources: Phylopic as listed in Acknowledgements and [91–94]. Arrows show direction of transcription where known. B, Phylogeny of *P. maximus* Hox and Parahox genes alongside those of known homology from previous work [95, 96] inferred using MrBayes (MrBayes, RRID:SCR_012067) [97] under the Jones model (1,000,000 generations, with 25% discarded as "burn-in") from a MAFFT alignment under the L-INS-I model [98]. Numbers at base of nodes are posterior probabilities, shown to 2 significant figures. Branches are coloured by gene.

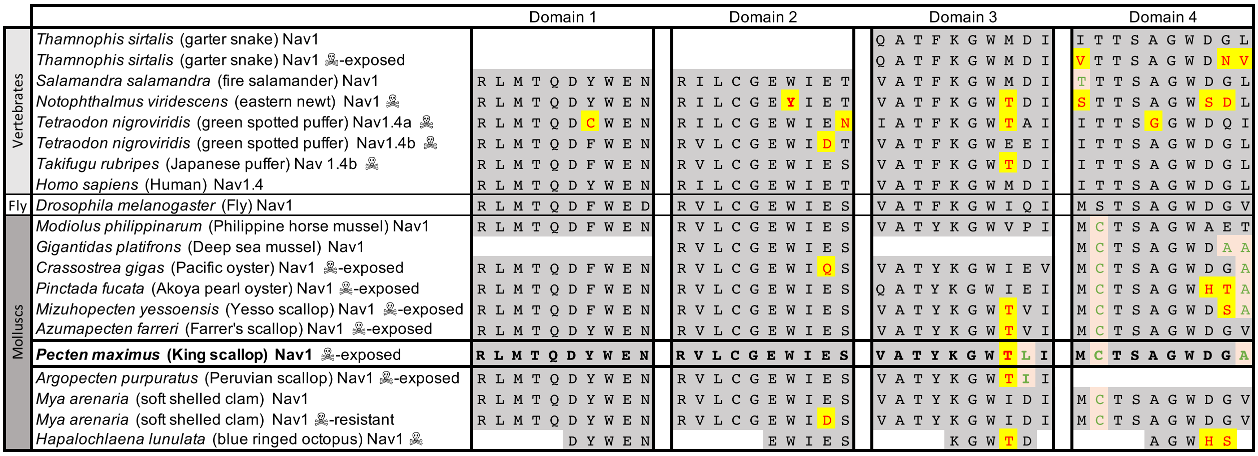

		Domain 1	Domain 2	Domain 3	Domain 4
Vertebrates	*Thamnophis sirtalis* (garter snake) Nav1			QATFKGWMDI	ITTSAGWDGL
	Thamnophis sirtalis (garter snake) Nav1 ☠-exposed			QATFKGWMDI	VTTSAGWDNV
	Salamandra salamandra (fire salamander) Nav1	RLMTQDYWEN	RILCGEWIET	VATFKGWMDI	TTTSAGWDGL
	Notophthalmus viridescens (eastern newt) Nav1 ☠	RLMTQDYWEN	RILCGEYIET	VATFKGWTDI	STTSAGWSDL
	Tetraodon nigroviridis (green spotted puffer) Nav1.4a ☠	RLMTQDCWEN	RILCGEWIEN	IATFKGWTAI	ITTSGGWDQI
	Tetraodon nigroviridis (green spotted puffer) Nav1.4b ☠	RLMTQDFWEN	RVLCGEWIDT	VATFKGWEEI	ITTSAGWDGL
	Takifugu rubripes (Japanese puffer) Nav 1.4b ☠	RLMTQDFWEN	RVLCGEWIES	VATFKGWTDI	ITTSAGWDGL
	Homo sapiens (Human) Nav1.4	RLMTQDYWEN	RILCGEWIET	VATFKGWMDI	ITTSAGWDGL
Fly	*Drosophila melanogaster* (Fly) Nav1	RLMTQDFWED	RVLCGEWIES	VATFKGWIQI	MSTSAGWDGV
Molluscs	*Modiolus philippinarum* (Philippine horse mussel) Nav1	RLMTQDFWEN	RVLCGEWIES	VATYKGWVPI	MCTSAGWAET
	Gigantidas platifrons (Deep sea mussel) Nav1		RVLCGEWIES		MCTSAGWDAA
	Crassostrea gigas (Pacific oyster) Nav1 ☠-exposed	RLMTQDFWEN	RVLCGEWIQS	VATYKGWIEV	MCTSAGWDGA
	Pinctada fucata (Akoya pearl oyster) Nav1 ☠-exposed	RLMTQDFWEN	RVLCGEWIES	QATYKGWIEI	MCTSAGWHTA
	Mizuhopecten yessoensis (Yesso scallop) Nav1 ☠-exposed	RLMTQDFWEN	RVLCGEWIES	VATYKGWTVI	MCTSAGWDSA
	Azumapecten farreri (Farrer's scallop) Nav1 ☠-exposed	RLMTQDYWEN	RVLCGEWIES	VATYKGWTVI	MCTSAGWDGV
	***Pecten maximus* (King scallop) Nav1** ☠-exposed	**RLMTQDYWEN**	**RVLCGEWIES**	**VATYKGWTLI**	**MCTSAGWDGA**
	Argopecten purpuratus (Peruvian scallop) Nav1 ☠-exposed	RLMTQDYWEN	RVLCGEWIES	VATYKGWTII	
	Mya arenaria (soft shelled clam) Nav1	RLMTQDYWEN	RVLCGEWIES	VATYKGWIDI	MCTSAGWDGV
	Mya arenaria (soft shelled clam) Nav1 ☠-resistant	RLMTQDYWEN	RVLCGEWIDS	VATYKGWIDI	MCTSAGWDGV
	Hapalochlaena lunulata (blue ringed octopus) Nav1 ☠	DYWEN	EWIES	KGWTD	AGWHS

Figure 5: Domain alignments (generated using MAFFT using the E-INS-I model [98]) of the sodium channel *Nav1* showing residues (text in red, highlighted in yellow) implicated in resistance to the neurotoxins tetrodotoxin (TTX) and saxitoxins (STX). Species of vertebrate and mollusc known to be resistant to TTX or STX [86–89] are shown alongside species and sub-populations with no resistance to these toxins. Species (and sub-populations) that produce or accumulate these toxins with little or no ill effect are marked with a skull-and-crossbones. *Pecten maximus* (bold text) shares a thymine residue in domain 3 known to confer neurotoxin resistance in several other species. It also has a number of residues (shown in green text with amber background) in Domains 3 and 4, which are either unique to *P. maximus* or shared with other resistant shellfish, but not seen in other species. These residues are good candidates for testing for a functional role in resistance in the future.

[9, 13]. A recent study, however, has shown that extracellular sodium concentration plays a crucial role in excitotoxicity of DA [99], suggesting that mutations that we observe at *Nav1* may also confer a degree of immunity to DA in *P. maximus*. This has ramifications for the study of neurotoxin resilience and prevalence in the increasingly important commercially fished populations of *P. maximus*.

Conclusions

The genome of *Pecten maximus* presented here is a well-assembled and annotated resource that will be of utility to a wide range of investigations in scallop, bivalve, and molluscan biology. It is, to date, the best-scaffolded genome available for bivalves, despite the heterozygosity seen in this clade. Given that this assembly is based on state-of-the-art long-range data and has undergone structural verification, this resource will be key for comparative analysis of structural variation and long-range synteny. The curated gene set of this species exhibits little loss compared to other sequenced bivalve species and possesses numerous duplicated genes, which have contributed to the largest gene set observed to date in molluscs. The genes are well annotated, with 88.2% of our high-confidence gene set mapped to a known gene. This genome has already yielded a range of insights into the biology of *P. maximus* and will provide a basis for investigations into fields such as physiology, neurotoxicology, population genetics, and shell formation for many years to come.

Availability of Supporting Data and Materials

The *Pecten maximus* xPecMax1.1 assembly is available at NCBI under the accession GCA_902652985.1. The data sets supporting the results of this article are available from FigShare [40], GigaDB [41], and also via the DNA Zoo website [55].

Additional Files

Supplementary File 1: Read quality assessment, FastQC/NanoComp
Supplementary File 2: Additional Blobplot plots and data, including those separated by phylum/superkingdom
Supplementary File 3: ReadsPerGene files output by STAR
Supplementary File 4: BLAST annotations, *Pecten maximus* gene models
Supplementary File 5: KEGG-KAAS annotations, *Pecten maximus* gene models

Abbreviations

AMPA: α-amino-3-hydroxy-5-methyl-4-isoxazolepropionic acid receptors; ASP: amnesiac shellfish poisoning; BLAST: Basic Local Alignment Search Tool; bp: base pairs; BUSCO: Benchmarking Universal Single Copy Orthologs; DA: domoic acid; Gb: gigabase pairs; GC: guanine-cytosine; KAAS: KEGG Automatic Annotation Server; KEGG: Kyoto Encyclopedia of Genes and Genomes; LINE: long interspersed nuclear element; LTR: long terminal repeat; MAFFT: Multiple Alignment using Fast Fourier Transform; Mb: megabase pairs; MIR: mammalian wide interspersed repeat; NDMA: N-methyl-D-aspartate receptors; NIH: National Institutes of Health; PacBio: Pacific Biosciences; PST: paralytic shellfish toxin; RNAseq: RNA sequencing; STX: saxitoxin; SINE: short interspersed nuclear element; TTX: tetrodotoxin; UTR: untranslated region; WGD: whole-genome duplication.

Competing Interests

The authors declare that they have no competing interests.

Funding

This work was performed as part of the Wellcome Sanger Institute 25 Genomes Project. Work on this manuscript was performed using funds from NHM DIF (SDR17012) to S.T.W. N.J.K. was supported by an H2020 MSCA grant during the conception of this study and thus this project received funding from the European Union's Horizon 2020 research and innovation programme under the Marie Sklodowska-Curie grant agreement No. 750,937. S.A.M. is supported by Wellcome grant WT207492. E.L.A. was supported by an NSF Physics Frontiers Center Award

(PHY1427654), the Welch Foundation (Q-1866), a USDA Agriculture and Food Research Initiative Grant (2017–05741), an NIH 4D Nucleome Grant (U01HL130010), and an NIH Encyclopedia of DNA Elements Mapping Center Award (UM1HG009375). Publication costs were paid with the support of the Marie Curie Alumni Association. Funding sources had no involvement in the decision to submit for publication.

Authors' Contributions

S.T.W. conceived of the study, provided the tissue samples, and contributed to the text. N.J.K. performed bioinformatic analyses, drafted the manuscript, and prepared the figures. S.A.M. assembled the draft genome. O.D., A.D.O., D.W., and E.L.A. generated and analysed the Hi-C data as part of the DNA Zoo effort. Y.R. and K.J. contributed to bioinformatic analyses, particularly RNAseq. K.H. led the assembly curation, with J.T. performing contamination checks and removal, Y.S. creating assembly analyses, and S.P. performing manual assembly curation. E.B., C.C., J.D., K.O., J.S., M.S., and A.W. aided with DNA extraction, processing, sequencing, and data delivery. D.M. and K.H. were responsible for project organization. All authors approved the final version of the manuscript.

Acknowledgements

We thank the members of the Riesgo and Williams laboratory groups for helpful discussions in preparation of this resource. We thank Phylopic, and particularly B. Duygu Özpolat and Taro Maeda for images in Fig. 4 (CC BY-NC-SA 3.0).

References

1. Vaughn CC, Hoellein TJ. Bivalve impacts in freshwater and marine ecosystems. Annu Rev Ecol Evol Syst 2018;**49**:183–208.
2. Brand AR. Scallop ecology: distributions and behaviour. In: Shumway SE, Parsons GJ , eds. Scallops: Biology, Ecology and Aquaculture. Elsevier; 2006:651–744.
3. Bates SS. Domoic-acid-producing diatoms: another genus added! J Phycol 2000;**36**:978–85.
4. Bell E, Lawler A, Masefield R, et al. Initial Assessment of Scallop Stock Status for Selected Waters Within the Channel 2016/2017. Centre for Environment Fisheries & Aquaculture Science; 2018:1–55.
5. Morvezen R, Charrier G, Boudry P, et al. Genetic structure of a commercially exploited bivalve, the great scallop *Pecten maximus*, along the European coasts. Conserv Genet 2015;**17**:57–67.
6. Strand O, Louro A, Duncan PF. European aquaculture. In: Shumway SE, Parsons GJ , eds. Scallops: Biology, Ecology, Aquaculture and Fisheries. Elsevier; 2016:859–90.
7. Thomas G, Gruffydd LD. The types of escape reactions elicited in the scallop *Pecten maximus* by selected sea-star species. Mar Biol 1971;**10**:87–93.
8. Land M. Image formation by a concave reflector in the eye of the scallop, *Pecten maximus*. J Physiol 1965;**179**:138–53.
9. Bejarano AC, VanDola FM, Gulland FM, et al. Production and toxicity of the marine biotoxin domoic acid and its effects on wildlife: a review. Hum Ecol Risk Assess 2008;**14**:544–67.
10. Beukers-Stewart B, Mosley M, Brand A. Population dynamics and predictions in the Isle of Man fishery for the great scallop, *Pecten maximus* L. ICES J Mar Sci 2003;**60**:224–42.
11. Spiro TG, Czernuszewicz RS, Li XY. Metalloporphyrin structure and dynamics from resonance raman spectroscopy. Coord Chem Rev 1990;**100**:541.
12. Bogan YM, Harkin AL, Gillespie J, et al. The influence of size on domoic acid concentration in king scallop, *Pecten maximus* (L.). Harmful Algae 2007;**6**:15–28.
13. Pulido OM. Domoic acid: biological effects and health implications. In: Rossini GP , ed. Toxins and Biologically Active Compounds from Microalgae. Vol. 2. Biological Effects and Risk Management. Modena, Italy: CRC; 2016:219–52.
14. Stommel EW, Mwatters MR. Marine neurotoxins: ingestible toxins. Curr Treat Options Neurol 2004;**6**:105–14.
15. Pulido OM. Domoic acid toxicologic pathology: a review. Mar Drugs 2008;**6**:180–219.
16. James K, Carey B, O'halloran J, et al. Shellfish toxicity: human health implications of marine algal toxins. Epidemiol Infect 2010;**138**:927–40.
17. Lefebvre KA, Silver MW, Coale SL, et al. Domoic acid in planktivorous fish in relation to toxic *Pseudo- nitzschia* cell densities. Mar Biol 2002;**140**:625–31.
18. Lefebvre KA, Robertson A. Domoic acid and human exposure risks: a review. Toxicon 2010;**56**:218–30.
19. Zhang G, Fang X, Guo X, et al. The oyster genome reveals stress adaptation and complexity of shell formation. Nature 2012;**490**:49–54.
20. Takeuchi T, Kawashima T, Koyanagi R, et al. Draft genome of the pearl oyster *Pinctada fucata*: a platform for understanding bivalve biology. DNA Res 2012;**19**:117–30.
21. Li Y, Sun X, Hu X, et al. Scallop genome reveals molecular adaptations to semi-sessile life and neurotoxins. Nat Commun 2017;**8**:1721.
22. Wang S, Zhang J, Jiao W, et al. Scallop genome provides insights into evolution of bilaterian karyotype and development. Nat Ecol Evol 2017;**1**:120.
23. Li C, Liu X, Liu B, et al. Draft genome of the Peruvian scallop *Argopecten purpuratus*. Gigascience 2018;**7**, doi:10.1093/gigascience/giy031.
24. Powell D, Subramanian S, Suwansa-Ard S, et al. The genome of the oyster *Saccostrea* offers insight into the environmental resilience of bivalves. DNA Res 2018;**25**: 655–65.
25. Gómez-Chiarri M, Warren WC, Guo X, et al. Developing tools for the study of molluscan immunity: the sequencing of the genome of the eastern oyster, *Crassostrea virginica*. Fish Shellfish Immunol 2015;**46**:2–4.
26. Murgarella M, Puiu D, Novoa B, et al. A first insight into the genome of the filter-feeder mussel *Mytilus galloprovincialis*. PLoS One 2016;**11**.
27. Uliano-Silva M, Dondero F, Dan Otto T, et al. A hybrid-hierarchical genome assembly strategy to sequence the invasive golden mussel, *Limnoperna fortunei*. Gigascience 2018;**7**, doi:10.1093/gigascience/gix128.
28. Sun J, Zhang Y, Xu T, et al. Adaptation to deep-sea chemosynthetic environments as revealed by mussel genomes. Nat Ecol Evol 2017;**1**:121.
29. Ran Z, Li Z, Yan X, et al. Chromosome-level genome assembly of the razor clam *Sinonovacula constricta* (Lamarck, 1818). Mol Ecol Resour 2019;**19**:1647–58.
30. Thai BT, Lee YP, Gan HM, et al. Whole genome assembly of the snout otter clam, *Lutraria rhynchaena*, using Nanopore and Illumina data, benchmarked against bivalve genome assemblies. Front Genet 2019;**10**.
31. Bai CM, Xin LS, Rosani U, et al. Chromosomal-level assembly of the blood clam, *Scapharca* (*Anadara*) *broughtonii*,

using long sequence reads and Hi-C. Gigascience 2019;**8**, doi:10.1093/gigascience/giz067.
32. Mun S, Kim YJ, Markkandan K, et al. The whole-genome and transcriptome of the manila clam (*Ruditapes philippinarum*). Genome Biol Evol 2017;**9**:1487–98.
33. Renaut S, Guerra D, Hoeh WR, et al. Genome survey of the freshwater mussel *Venustaconcha ellipsiformis* (Bivalvia: Unionida) using a hybrid de novo assembly approach. Genome Biol Evol 2018;**10**:1637–46.
34. Calcino AD, de Oliveira AL, Simakov O, et al. The quagga mussel genome and the evolution of freshwater tolerance. DNA Res 2019;**26**:411–22.
35. McCartney MA, Auch B, Kono T, et al. The genome of the zebra mussel, ”*Dreissena polymorpha*”: a resource for invasive species research. bioRxiv 2019:696732, doi:10.1101/696732.
36. Takeuchi T, Koyanagi R, Gyoja F, et al. Bivalve-specific gene expansion in the pearl oyster genome: implications of adaptation to a sessile lifestyle. Zool Lett 2016;**2**:3.
37. Gonzalez VL, Andrade SC, Bieler R, et al. A phylogenetic backbone for Bivalvia: an RNA-seq approach. Proc Biol Sci 2015;**282**:20142332.
38. De Coster W, D’Hert S, Schultz DT, et al. NanoPack: visualizing and processing long-read sequencing data. Bioinformatics 2018;**34**:2666–9.
39. Andrews S. FastQC: a quality control tool for high throughput sequence data. Cambridge, United Kingdom: Babraham Bioinformatics, Babraham Institute; 2010.
40. Kenny NJ. *Pecten maximus* genome, gene models, annotations and related files. Figshare 2019, doi:10.6084/m9.figshare.10311068.v3.
41. Kenny NJ, McCarthy S, Dudchenko O, et al. Supporting data for “The gene-rich genome of the scallop *Pecten maximus*.” GigaScience Database 2020. http://dx.doi.org/10.5524/100726
42. Ruan J, Li H. Fast and accurate long-read assembly with wtdbg2. Nat Methods 2020;**17**:155–8.
43. Garrison E, Marth G. Haplotype-based variant detection from short-read sequencing. arXiv 2012:1207.3907.
44. vgp-assembly pipeline. freebayes polish tool. https://github.com/VGP/vgp-assembly/tree/master/pipeline/freebayes-polish. Accessed 14 April 2020.
45. WTSI-HPAG. Scaff10X assembly tool. https://github.com/wtsi-hpag/Scaff10X. Accessed 14 April 2020.
46. Dudchenko O, Batra SS, Omer AD, et al. De novo assembly of the *Aedes aegypti* genome using Hi-C yields chromosome-length scaffolds. Science 2017;**356**:92.
47. Dudchenko O, Shamim MS, Batra SS, et al. The Juicebox Assembly Tools module facilitates de novo assembly of mammalian genomes with chromosome-length scaffolds for under $1000. bioRxiv 2018:254797.
48. Chow W, Brugger K, Caccamo M, et al. gEVAL—a web-based browser for evaluating genome assemblies. Bioinformatics 2016;**32**:2508–10.
49. Ranallo-Benavidez TR, Jaron KS, Schatz MC. GenomeScope 2.0 and Smudgeplot for reference-free profiling of polyploid genomes. Nature Communications 2020;**11**(1):1–10.
50. Laetsch DR, Blaxter ML. BlobTools: Interrogation of genome assemblies. F1000Res 2017;**6**:1287.
51. xPecMax1.1. *Pecten maximus*Juicebox plot. http://bit.ly/2QaYqvk. Accessed 14 April 2020.
52. Insua A, Lopez-Pinon MJ, Freire R, et al. Karyotype and chromosomal location of 18S-28S and 5S ribosomal DNA in the scallops *Pecten maximus* and *Mimachlamys varia* (Bivalvia: Pectinidae). Genetica 2006;**126**:291–301.
53. Altschul SF, Gish W, Miller W, et al. Basic Local Alignment Search Tool. J Mol Biol 1990;**215**:403–10.
54. Robinson JT, Turner D, Durand NC, et al. Juicebox.js provides a cloud-based visualization system for Hi-C data. Cell Syst 2018;**6**:256–258.e251.
55. DNA Zoo. Great scallop (*Pecten maximus*). https://www.dnazoo.org/assemblies/Pecten_maximus. Accessed 24 March 2020.
56. Rodríguez-Juíz A, Torrado M, Méndez J. Genome-size variation in bivalve molluscs determined by flow cytometry. Mar Biol 1996;**126**:489–97.
57. Vurture GW, Sedlazeck FJ, Nattestad M, et al. GenomeScope: fast reference-free genome profiling from short reads. Bioinformatics 2017;**33**:2202–4.
58. Li H. Minimap2: pairwise alignment for nucleotide sequences. Bioinformatics 2018;**34**:3094–100.
59. Yoshida M-A, Ishikura Y, Moritaki T, et al. Genome structure analysis of molluscs revealed whole genome duplication and lineage specific repeat variation. Gene 2011;**483**:63–71.
60. Solé-Cava AM, Thorpe JP. High levels of genetic variation in natural populations of marine lower invertebrates. Biol J Linn Soc 1991;**44**:65–80.
61. Biscotti MA, Barucca M, Canapa A. New insights into the genome repetitive fraction of the Antarctic bivalve *Adamussium colbecki*. PLoS One 2018;**13**:e0194502.
62. Tarailo-Graovac M, Chen N. Using RepeatMasker to identify repetitive elements in genomic sequences. Curr Protoc Bioinformatics 2009:Chapter 4:Unit 4 10.
63. Hoff KJ, Stanke M. WebAUGUSTUS–a web service for training AUGUSTUS and predicting genes in eukaryotes. Nucleic Acids Res 2013;**41**:W123–8.
64. Artigaud S, Thorne MA, Richard J, et al. Deep sequencing of the mantle transcriptome of the great scallop *Pecten maximus*. Mar Genomics 2014;**15**:3–4.
65. Pauletto M, Milan M, Huvet A, et al. Transcriptomic features of *Pecten maximus* oocyte quality and maturation. PLoS One 2017;**12**:e0172805.
66. Krueger F. Trim Galore: a wrapper tool around Cutadapt and FastQC. 2012. http://www.bioinformatics.babraham.ac.uk/projects/trim_galore/. Accessed 14 April 2020.
67. Haas BJ, Papanicolaou A, Yassour M, et al. De novo transcript sequence reconstruction from RNA-seq using the Trinity platform for reference generation and analysis. Nat Protoc 2013;**8**:1494.
68. Smith-Unna R, Boursnell C, Patro R, et al. TransRate: reference-free quality assessment of de novo transcriptome assemblies. Genome Res 2016;**26**:1134–44.
69. Li B, Fillmore N, Bai Y, et al. Evaluation of de novo transcriptome assemblies from RNA-Seq data. Genome Biol 2014;**15**:553.
70. Li W, Godzik A. Cd-hit: a fast program for clustering and comparing large sets of protein or nucleotide sequences. Bioinformatics 2006;**22**:1658–9.
71. Kent WJ. BLAT—the BLAST-like alignment tool. Genome Res 2002;**12**:656–64.
72. Sun J, Mu H, Ip JCH, et al. Signatures of divergence, invasiveness, and terrestrialization revealed by four apple snail genomes. Mol Biol Evol 2019;**36**:1507–20.
73. Buchfink B, Xie C, Huson DH. Fast and sensitive protein alignment using DIAMOND. Nat Methods 2015;**12**:59–60.
74. Du X, Song K, Wang J, et al. Draft genome and SNPs associated with carotenoid accumulation in adductor muscles of bay scallop (*Argopecten irradians*). J Genomics 2017;**5**:83–90.
75. Dobin A, Davis CA, Schlesinger F, et al. STAR: ultrafast universal RNA-seq aligner. Bioinformatics 2013;**29**:15–21.

76. Simão FA, Waterhouse RM, Ioannidis P, Kriventseva EV, Zdobnov EM. BUSCO: assessing genome assembly and annotation completeness with single-copy orthologs. Bioinformatics 2015;**31**(19):3210–2.
77. Lemer S, Gonzalez VL, Bieler R, et al. Cementing mussels to oysters in the pteriomorphian tree: a phylogenomic approach. Proc Biol Sci 2016;**283**:20160857.
78. Crow KD, Smith CD, Cheng JF, et al. An independent genome duplication inferred from Hox paralogs in the American paddlefish–a representative basal ray-finned fish and important comparative reference. Genome Biol Evol 2012;**4**: 937–53.
79. Leite DJ, Baudouin-Gonzalez L, Iwasaki-Yokozawa S, et al. Homeobox gene duplication and divergence in arachnids. Mol Biol Evol 2018:352240.
80. Duncan PF, Brand AR, Strand O, et al. The European scallop fisheries for *Pecten maximus*, *Aequipecten opercularis*, *Chlamys islandica* and *Mimachlamys varia*. In: Shumway SE, Parsons GJ, eds. Scallops: Biology, Ecology, Aquaculture and Fisheries. Cambridge, MA: Elsevier; 2016:781–858.
81. Shumway SE, Cembella AD. The impact of toxic algae on scallop culture and fisheries. Rev Fish Sci 1993;**1**:121–50.
82. Emms DM, Kelly S. OrthoFinder: phylogenetic orthology inference for comparative genomics. Genome biology 2019;**20**(1):1–14.
83. Cusick KD, Sayler GS. An overview on the marine neurotoxin, saxitoxin: genetics, molecular targets, methods of detection and ecological functions. Mar Drugs 2013;**11**:991–1018.
84. Bricelj VM, Connell L, Konoki K, et al. Sodium channel mutation leading to saxitoxin resistance in clams increases risk of PSP. Nature 2005;**434**:763–7.
85. Roncalli V, Lenz PH, Cieslak MC, et al. Complementary mechanisms for neurotoxin resistance in a copepod. Sci Rep 2017;**7**:14201.
86. Kontis KJ, Goldin AL. Site-directed mutagenesis of the putative pore region of the rat IIA sodium channel. Mol Pharmacol 1993;**43**:635–44.
87. Choudhary G, Yotsu-Yamashita M, Shang L, et al. Interactions of the C-11 hydroxyl of tetrodotoxin with the sodium channel outer vestibule. Biophys J 2003;**84**:287–94.
88. Yotsu-Yamashita M, Nishimori K, Nitanai Y, et al. Binding properties of 3H-PbTx-3 and 3H-saxitoxin to brain membranes and to skeletal muscle membranes of puffer fish *Fugu pardalis* and the primary structure of a voltage-gated Na+ channel α-subunit (fMNa1) from skeletal muscle of *F. pardalis*. Biochem Biophys Res Commun 2000;**267**:403–12.
89. Hanifin CT, Gilly WF. Evolutionary history of a complex adaptation: tetrodotoxin resistance in salamanders. Evolution 2015;**69**:232–44.
90. Geffeney SL, Williams BL, Rosenthal JJC, et al. Convergent and parallel evolution in a voltage-gated sodium channel underlies TTX-resistance in the greater blue-ringed octopus: *Hapalochlaena lunulata*. Toxicon 2019;**170**:77–84.
91. Comstock JH. A manual for the study of insects. Ithaca, New York: Comstock Pub. Co.; 1895.
92. Lear E. Alphabet of Nonsense. Unpublished artwork, 1860.
93. Mather F, The Scallop. Popular Science Monthly 1896;**49**:544.
94. Gosse PH. Natural History (Mollusca). London: Society for Promoting Christian Knowledge; 1854.
95. Simakov O, Marletaz F, Cho SJ, et al. Insights into bilaterian evolution from three spiralian genomes. Nature 2013;**493**:526–31.
96. Huan P, Wang Q, Tan S, et al. Dorsoventral dissociation of Hox gene expression underpins the diversification of molluscs. bioRxiv 2019; p.603092.
97. Huelsenbeck JP, Ronquist F. MRBAYES: Bayesian inference of phylogenetic trees. Bioinformatics 2001;**17**:754–5.
98. Katoh K, Rozewicki J, Yamada KD. MAFFT online service: multiple sequence alignment, interactive sequence choice and visualization. Brief Bioinform 2019;**20**:1160–6.
99. Perez-Gomez A, Cabrera-Garcia D, Warm D, et al. From the cover: selective enhancement of domoic acid toxicity in primary cultures of cerebellar granule cells by lowering extracellular Na+ concentration. Toxicol Sci 2018;**161**:103–14.